1932-4510/08/$25.00©2008IEEE

IN SYNOPSIS, THE SURFACE PLASMON polariton (SPP) is introduced as a waveguide mode that requires only a single interface. It is shown that nanostructuring can be used to reduce the SPP wavelength and group velocity and thereby provide enhanced field intensities and extreme subwavelength optical confinement. Localized surface plasmons (LSPs) of metal particles are analyzed using the quasi-static approximation. It is shown that LSPs can be used to create electromagnetic field enhancements. Finally, applications of surface plasmon nanophotonics are highlighted, including surface plasmon resonance sensing, surface-enhanced Raman spectroscopy, enhanced fluorescence, nonlinear optics, near-field imaging and subwavelength lithography, and optical trapping and manipulation.

Early work on radiating dipoles at the earth's surface led to surface wave solutions [1]. Later, it was discovered that such surface waves played an important role in electron energy loss at metal surfaces [2]. All-optical coupling to these surface plasmon waves was demonstrated by attenuated total-internal reflection (ATR) [3], and this geometry plays an important role in contemporary surface-binding optical sensors. Surface-sensing technologies make use of exponentially bound surface plasmons within an optical wavelength of the surface.

Surface plasmons allow for strong optical field enhancement at the metal interface, which can be used to enhance weak optical processes, like second harmonic generation [4]. Electromagnetic field enhancements can be even greater for nanostructured metals where the light is efficiently concentrated at the subwavelength scale. Such enhancement has allowed for observations of surface-enhanced Raman scattering (SERS) at the single-molecule level from randomly roughened surfaces [5]–[7], while conventional Raman scattering is much weaker than fluorescence. Similar enhancements have been observed from roughened metal surfaces for other weak optical processes, such as second-harmonic generation [8].

In recent years, nanofabrication technology has advanced signficantly, both for top-down methods like electron-beam lithography and focused-ion beam milling, and bottom-up methods like nanoparticle assembly and ordered anodic pore formation. With these improvements in nanofabrication, there have been rapid advancements in surface plasmon nanophotonics because, for the first time, it is possible to reliably control light at the nanoscale. The scientific community is now harnessing the potential of surface plamsons to bring light to the nanometer scale.

The purpose of this tutorial is to give practical introduction to surface plasmon nanophotonics. SPPs will be introduced as a waveguide mode at a single interface. It will be shown how SPPs in nanostructures can both concentrate the local field intensity and shorten the optical wavelength. LSPs will be introduced and described using the quasi-static approximation. It

Surface Plasmon Nanophotonics: A Tutorial

Improvements in nanofabrication lead to rapid advancements in surface plasmon nanophotonics.

REUVEN GORDON

Digital Object Identifier 10.1109/MNANO.2008.931481

will be shown how LSPs lead to local field enhancement, which may be further cascaded to achieve additional enhancement. A brief discussion of six application areas of surface plasmon nanophotonics will be given: surface plasmon resonance (SPR) sensing, SERS, enhanced fluorescence, nonlinear optics, nanolithography and subwavelength imaging, and optical trapping.

SURFACE PLASMON POLARITONS

SPPs AS A WAVEGUIDE MODE

SPPs are commonly described as electromagnetic waves formed by charge oscillations at the surface of a metal. Figure 1(a) shows a popular schematic, which is useful for visualizing the SPP. We see many interesting features from this figure: the electrons in the metal have moved to create positive and negative charge distributions and electric field polarization. The term "polariton" refers to a wave of polarizations, positive and negative charges in a row. The electric field normal to the surface is out-of-phase by $\pi/2$ with respect to the electric field parallel to the surface. The wave has a transverse magnetic component. This figure is not useful, however, in answering why there is such a wave at the surface. What conditions are required for this wave to exist? How does it propagate?

The SPP is a waveguide mode. In a dielectric slab waveguide, light is kept within a high refractive index core by total-internal reflection. The self-consistency condition for the waveguide modes is that the round-trip phase of the mode is a multiple of 2π, including the phase-of-reflection and of propagation. This is required so that the transverse field distribution does not change with propagation. Metals can satisfy the self-consistency condition with only a single interface because some metals have a negative relative permittivity in the visible regime. This means that the normal component of the electric field changes sign when crossing the interface—the normal component of the electric displacement is continuous at the boundary. This sign-change is equivalent to a phase-shift of π; when crossing the interface twice, the total phase-shift is 2π and the self-consistency condition is naturally satisfied. Thereby, a metal-dielectric interface can sustain a waveguide mode. Figure 1(b) shows this phase-shift schematically.

Solving Maxwell's equations with exponential solutions decaying away from the interface and propagation in the plane of the interface gives the form of the y-component of the SPP magnetic field:

$$H_y(x,z,t) = \begin{cases} \exp(-\gamma_d x + i\beta z - i\omega t) & x > 0 \\ \exp(\gamma_m x + i\beta z - i\omega t) & x < 0 \end{cases} \quad (1)$$

with:

$$\gamma_{m,d} = \frac{\omega}{c}\sqrt{\frac{-\varepsilon_{m,d}^2}{\varepsilon_m + \varepsilon_d}} \quad (2)$$

and

$$\beta = \frac{\omega}{c}\sqrt{\frac{\varepsilon_m \varepsilon_d}{\varepsilon_m + \varepsilon_d}} \quad (3)$$

where $i = \sqrt{-1}$, $\omega = 2\pi f$ is the angular frequency of light, c is the speed of light in vacuum, ε_m is the relative permittivity of the metal and ε_d is the relative permittivity of the dielectric. This equation describes a waveguide mode for $\varepsilon_m < -\varepsilon_d$, ignoring the typically smaller imaginary contributions that lead to loss. [Loss can be captured by the imaginary part of the propagation constant in (3)]. The remaining electric field components can be found by using the Ampère-Maxwell equation. The optical properties of metals have been considered in detail in past works (e.g., [9] and [10]). Figure 1(c) shows the transverse magnetic field of the SPP. The SPP is a TM waveguide mode.

The propagation constant of the SPP gives an effective index, $n_{\text{eff}} = c\beta/\omega$, that is greater than the refractive index of the dielectric. In other words, the SPP has a shorter wavelength than plane-waves in the dielectric. This means that the SPP waveguide mode is not coupled to free-space plane-waves; just as light inside a fiber-optic cable stays inside the fiber. In both cases, we can add a prism or a grating to couple plane waves to the SPP or to the waveguide mode inside an optical fiber by a process of phase-matching (simultaneous momentum and energy conservation).

SPPs IN NANOSTRUCTURES

To understand the influence that nanostructuring can have on light with the help of surface plasmons, we consider the most straightforward nanostructure: a gap between two metals. Figure 2(a) shows the metal-insulator-metal (MIM) gap. The solution to the gap is equivalent to the TM dielectric waveguide, except that the relative permittivities of the cladding layers are negative and the transverse magnetic field has a hyperbolic cosine dependence inside the gap. The equation to find the solution for the effective index of the MIM waveguide mode is

$$\tanh\left(\frac{d}{2}\sqrt{\beta^2 - \left(\frac{\omega}{c}\right)^2 \varepsilon_d}\right) = -\frac{\varepsilon_d}{\varepsilon_m}\sqrt{\frac{\beta^2 - \left(\frac{\omega}{c}\right)^2 \varepsilon_m}{\beta^2 - \left(\frac{\omega}{c}\right)^2 \varepsilon_d}} \quad (4)$$

Figure 2(b) plots the effective index of the MIM waveguide mode as a function of gap width, d, for two different wavelengths. Two important results can be seen from this figure:

1) As d is made small, the effective index becomes large. In other words, the phase velocity slows down and the wavelength becomes smaller: we can make light "smaller" by making the gap smaller. This has many interesting effects. For example, if you want to increase the cut-off wavelength of a rectangular hole in a metal, it is better to squeeze the hole in the vertical direction, rather than making it larger [11].
2) As d is made smaller, the group index increases; light is slowing down as we make the MIM gap narrower. Therefore, if we gradually taper the gap to a point, light will slow down as it progresses, and so the energy will build up (provided that loss is sufficiently small and the taper is adiabatic to minimize reflection). Strong field enhancement due to slowing-down of the surface plasmon has been demonstrated at a metal tip where the dielectric surrounds the metal [12].

From this, we see that two important advantages of metal nanostructures:

1) Shrinking the optical wavelength
2) Enhancing the local field intensity.

LOCALIZED SURFACE PLASMONS

LSPs are charge oscillations that are bound to a small metal particle or nanostructure. These oscillations can be represented by the displacement of charge in the sphere. How can we understand the important effects of LSPs?

For very small particles, where the spatial variation of the electromagnetic field is confined to lengths much smaller than the optical wavelength, the time-dependent contributions to Maxwell's equations may be neglected, so that the solution to the field distribution becomes the same as the electrostatic solution [13]. For example, for a metal sphere in a dielectric, the field inside the metal is given by:

$$E_{\text{in}} = \frac{3\varepsilon_d E_o}{\varepsilon_m + 2\varepsilon_d} \qquad (5)$$

where E_o is the electric field away from the sphere (which contains the time-dependence in the quasi-static approximation). Ignoring the imaginary contributions to the relative permittivities in Equation (5), it is clear that the field inside the sphere diverges when $\varepsilon_m = -2\varepsilon_d$. Considering continuity of the parallel component of the electric field at the boundary, this leads to a strong enhancement of the field on the outer surface of the sphere, which is limited in practice by the imaginary part of ε_m. (For a more accurate theory, it should be kept in mind that the bulk permittivities of metals are less accurate for small particles because of electron scattering at the boundaries of the particle [14]). In keeping with the quasistatic approximation, we see that the resonance is independent of particle size, but this is not the case for larger particles. Changing the particle-shape can influence the resonances as well. The LSP-enhanced field goes hand-in-hand with an enhanced local dipole, and so the scattered light will be greatest near the resonance. For a single particle, the quality of the resonance is limited by the dispersion of the metal and dielectric, as is clear from the field enhancement denominator in (5).

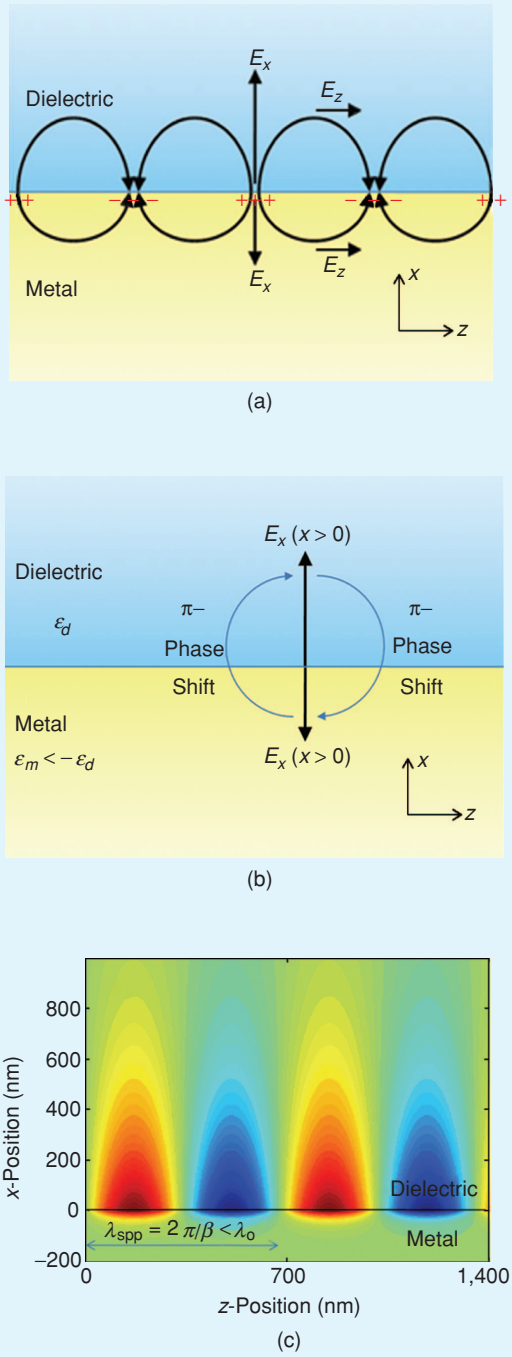

FIGURE 1 (a) Schematic representation of SPP as charge oscillations at the interface between a metal and a dielectric. The electric field has a longitudinal (z-direction) component that is $\pi/2$ out-of-phase with the transverse component (x-direction). (b) Schematic of SPP self-consistency relation that is allowed for by a negative relative permittivity in the metal. The electromagnetic wave has a π phase-shift upon crossing the boundary, allowing for self-consistency when crossing the boundary twice. This allows the SPP waveguide mode to exist at only a single interface. (c) Calculated transverse magnetic field (y-direction) for an SPP above gold at free-space wavelength of 700 nm. The SPP wavelength is shorter than the free-space wavelength, as described in the text.

It is clear that the field at surface of a nanoparticle is enhanced with respect to incident field. If we cascade this effect, with smaller and smaller particles in close proximity, the total increase in the local electromagnetic field can be made very large. For example, electric field enhancements of over 1,000 have been calculated for self-similar spherical particles in a row [15].

It is also possible to get LSPs from holes or slits in metals since the light inside the hole will be reflected at each end (due impedance and geometric mismatch), leading to standing waves that are localized in the hole, commonly referred to as Fabry-Perot resonances [16].

APPLICATIONS

SURFACE PLASMON RESONANCE SENSING

SPPs are evanescently bound to the metal surface and they are sensitive to dielectric perturbations at the surface. Consequently, metals can be used to sense the binding of molecules to the surface in a technique

called SPR sensing. ATR, also known as the Kretschmann geometry, is the most common method for SPR. It uses phase-matched evanescent coupling between propagating light in a high refractive index medium and the SPP. The phase matching is controlled by tuning the angle and/or wavelength of the incident beam. For the phase-matched condition, light is transferred to the SPP and so there is increased loss (from the metal) and reduced reflection.

Figure 3(a) shows the geometry of an ATR sensor. Figure 3(b) shows the reflection as a function of incidence angle when the refractive index of a 5 nm surface layer is modified to 1.5 (from 1.33 of the aqueous surrounding medium). The shift in the reflection minimum (in this case 0.7°) is used to sense the absorption of molecules at the surface. The Appendix provides a simple Matlab script used to calculate this ATR reflection curve. It is important to include the loss of the metal in this calculation, otherwise all the light that is coupled into the SPP is coupled out of it once again and so the reflection is always 100%.

SPR has applications in drug development, medical diagnostics, environmental monitoring, food and water safety [17]. The ATR SPR sensitivity is $\sim 10^{-7}$ refractive index units (RIU) (i.e., the 7th significant figure after the decimal in refractive index), and limit of detection is ~10 pg/mL.

As described previously, the LSP resonance is sensitive to the local refractive index, and LSPs have been studied for applications to SPR sensing as well [18]. One advantage of LSPs is that the sensing volume is reduced to the local environment and so a smaller limit of detection and greater multiplexing are possible.

SURFACE-ENHANCED RAMAN SPECTROSCOPY

In Raman scattering, a photon is scattered by a material with increased (or decreased) energy due to the simultaneous absorption (or emission) of a phonon (vibration mode) in the material. Raman scattering provides the phonon energy spectrum of the material; therefore, it is a useful spectroscopic method for identifying materials by their vibrational "fingerprint." Raman scattering is weak—typically 14 orders of magnitude weaker than fluorescence. Therefore, we are interested in enhancing Raman scattering to routinely characterize materials down to the single-molecule level.

SERS makes use of local field enhancements provided by metal nanostructures. The metal nanostructures focus light down to the nanoscale and enhance the local field. While this enhancement alone would usually only provide a linear increase in the Raman scattering intensity, the metal nanostructure also works in reverse to efficiently capture the Raman-scattered photons and direct them to the detector. This double-enhancement can occur because the Raman scattered photon has almost the same energy as the incident photon—the phonon energy is relatively small. The double-enhancement increases the Raman-scattering intensity by the square of the near-field intensity enhancement, even though Raman scattering is linear (in photon number). In terms of the electric field, a metal nanostructure that provides 3,000 times enhancement gives the required 14 orders of magnitude increase in Raman scattering to obtain signal at the single-molecule level.

While early observations of SERS at the single molecule level used randomly nanostructured metal surfaces [5], [6], there is great potential for tailor-made nanostructures to provide more predictable field enhancements. With tailor-made nanostructures, it is possible to design the location of field enhancement, the magnitude of field enhancement and the wavelengths that provide field enhancement.

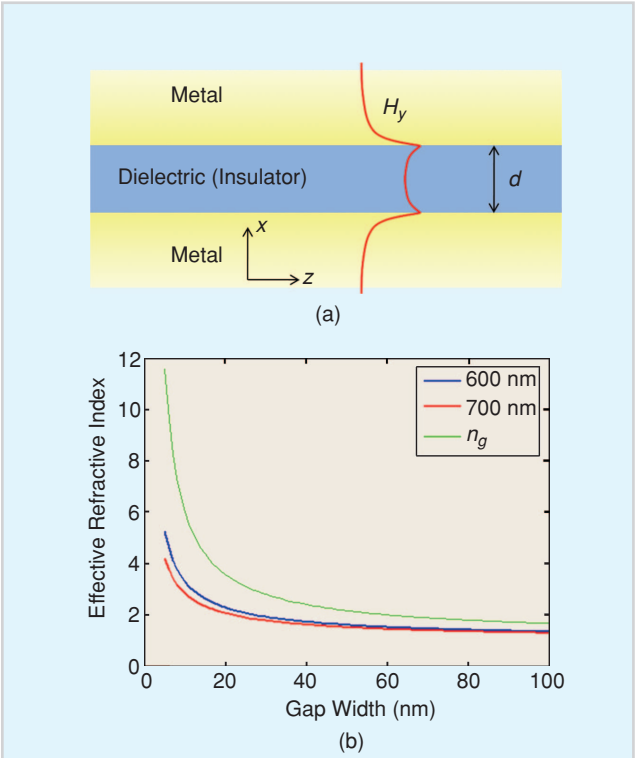

FIGURE 2 (a) Schematic of MIM structure with gap d. Transverse magnetic field is shown in red, which has a hyperbolic cosine dependence in the gap an exponential decay into the metal. (b) Effective refractive index of waveguide mode within MIM gap, which decreases as the gap is made smaller. Calculations for two free-space wavelengths are shown using the relative permittivity of gold and the difference is used to estimate the group index, which also increases as the gap is made smaller. Therefore, the light slows down as the gap is made smaller.

ENHANCED FLUORESCENCE AND ABSORPTION

As with Raman scattering, the presence of a nanostructured metal can modify the local electromagnetic environment around a molecule. This modification is commonly expressed by the Purcell factor, and it essentially means that the optical interaction with the material is enhanced by some factor. As a result, fluorescence (and other optical processes, such as absorption) can be enhanced by metal nanostructures. The disadvantage is that often the light can be strongly coupled to surface plasmons so that it is

absorbed before it is extracted (since metals are lossy). Enhanced absorption using nanostructured metals is presently of interest for harvesting solar energy more efficiently [19].

NONLINEAR OPTICS

As nonlinear optics is typically weak and it scales nonlinearly with the electromagnetic field, there is a clear benefit from the extreme subwavelength focusing allowed by surface plasmon nanophotonics. Strong nonlinear enhancements are possible in metal composite materials, or nanostructured metal surfaces. Other opportunities exist, such as using SPP/LSP resonances together to enhance different wavelengths simultaneously in frequency conversion nonlinear optics. For example, a recent work showed enhanced second harmonic generation of nanohole arrays in a metal film by matching the fundamental wavelength to the SPP resonance and the second harmonic (at half the free-space wavelength of the fundamental) to the LSP resonance [20].

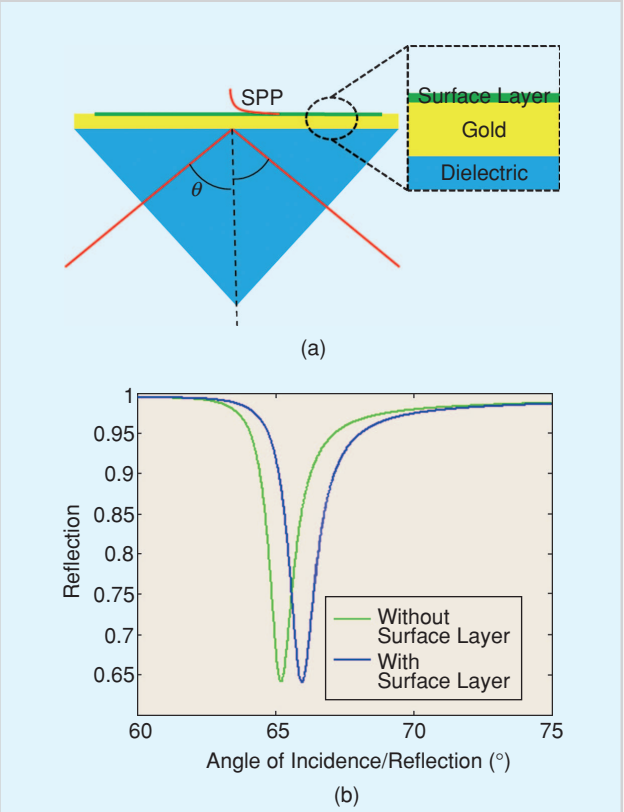

FIGURE 3 (a) Schematic of ATR configuration for SPR sensing. The ATR configuration couples plane-waves inside the prism into SPP waves when the angle and wavelength are tuned to the phase-matching condition. Since the SPP has loss, the reflection is reduced when there is coupling to the SPP wave. (b) Calculated SPR reflection for a 50 nm gold layer at free-space wavelength of 632 nm, with and without a 5 nm surface layer of refractive index 1.5. (It is assumed that above the surface layer is water, with refractive index 1.33). The shift in the reflection dip is used to detect the surface layer.

NANOLITHOGRAPHY AND SUBWAVELENGTH IMAGING

Surface plasmons can be used to shrink the optical wavelength (particularly in metal nanostructures). They can also be used to recapture evanescent waves that are lost in conventional imaging, which is the origin of the diffraction limit. Therefore, it is natural to apply nanostructured metals to nanolithography and subwavelength imaging. It has been shown that operating in the flat region of the plasmon dispersion can give rise to a poor man's perfect lens in the optical regime—this is basically operating close to the LSP resonance of a thin film [21], [22]. There is great research potential for using metal nanostructures to achieve extreme subwavelength focusing [23].

OPTICAL TRAPPING AND MANIPULATION

A photon scattered by a particle imparts momentum to that particle, which can be used for trapping and for manipulation. Optical trapping depends upon the gradient of the electric field intensity [24]. Optical trapping of nanometer-sized particles is especially difficult since the Rayleigh scattering that creates the trap scales as the fourth power of particle size. In addition, the random particle motion from diffusion acts against the trapping and this scales inversely to the particle size. Therefore, the overall trapping ability decreases as the fifth power of the particle size, which makes trapping of nanometer-scale particles extremely difficult. Since nanostructured metals allow for strong field intensity gradients, they are promising candidates for trapping and manipulation of nanometer particles. Recent demonstrations have shown particle trapping by using metal disks [25] and nanoantennae. This research area has potential to allow for trapping in the study of nanometer-sized objects, such as DNA and viruses.

CONCLUSIONS AND OUTLOOK

In this tutorial, the underlying principles of surface plasmon nanophotonics have been demonstrated. It is clear that metal nanostructures offer great promise by bringing light to the nanoscale and thereby enhancing optical interactions with materials. Many applications naturally benefit from this approach, as were described in this tutorial.

In recent years there has been great progress in surface plasmon nanophotonics, mainly because of improvements in:

1) the control of the material science for the creation of metal nanostructure particles and patterned nanostructured templates
2) methods for creating metal nanostructures by optical lithography [26], [27], ion-beam milling and electron beam lithography
3) electromagnetic calculation tools and computational power, which are capable of capturing the realistic dispersion of metals, for example, by using finite-difference time-domain methods on parallelized computer clusters.

Each of these factors has made the field of surface plasmon nanophotonics accessible to researchers worldwide and there will likely be increased activity and more breakthroughs in this field for years to come.

REFERENCES

[1] A. Sommerfeld, "Über die ausberitung der wellen in der drahtlosen telegraphie," *Ann. Phys.*, vol. 28, no. 4, pp. 665–736, 1909.

APPENDIX

The ATR of a multilayer system can be calculated by assuming two bidirectional plane-waves as solutions for each layer. These plane waves have amplitude coefficients that are solved by matching the boundary-conditions at the interface of each layer. For ATR, the top surface electric field is an exponentially bound wave (arbitrarily set to unity), and the implausible exponentially growing wave is set to zero. Then it only remains to match the field at each layer and propagate to the next layer (in the y-direction) using the wave-vector for that layer. A Matlab script for this calculation is given below.

```
% Matlab script to calculate ATR-SPR reflection

% refractive indices of layers, substrate is last
n = [1.33 1.5 sqrt(-15 + 0.1*i) 1.56];

% thickness of middle layers normalized to free-space wavelength
% even though infinite, the first and last layers are set to zero
d = [0 5 50 0]/632;

% angle of incidence in substrate (in radians)
theta = pi/180*40;

% wavevectors in units of inverse free-space wavelength
k_x = 2*pi*n(length(n))*sin(theta);
k_y = sqrt((2*pi*n).^2 - k_x^2);

% a and b are the coefficients of the magnetic field amplitude
% in top layer, decaying evanescent field only, amplitude set to unity
a(1) = 0;
b(1) = 1;

% match boundary conditions and propagate through each layer
for m = 2:length(n)

a(m) = ((a(m-1) + b(m-1)) + k_y(m-1)/k_y(m)*(n(m)/n(m - 1))^2*(a(m-1)-
    b(m - 1)))/2*exp(i*k_y(m)*d(m));

b(m) = ((a(m-1) + b(m-1)) - k_y(m-1)/k_y(m)*(n(m)/n(m - 1))^2*(a(m-1)-
b(m - 1)))/2*exp(-i*k_y(m)*d(m));

end

%reflection for the angle theta
r = abs(a(length(n))/b(length(n)))^2;
```


[2] R.H. Ritchie, "Plasma losses by fast electrons in thin films," *Phys. Rev.*, vol. 106, no. 5, pp. 874–881, June 1957.

[3] E. Kretschmann, "Die Bestimmung optischer Konstanten von Metallen durch Anregung von Oberflächenplasmaschwingungen," *Zeitschrift für Physik A Hadrons and Nuclei*, vol. 241, no. 4, pp. 313–324, Aug. 1971.

[4] H.J. Simon, D.E. Mitchell, and J.G. Watson, "Optical second-harmonic generation with surface plasmons in silver films," *Phys. Rev. Lett.*, vol. 33, no. 26, pp. 1531–1534, Dec. 1974.

[5] K. Kneipp, Y. Wang, H. Kneipp, L.T. Perelman, I. Itzkan, R.R. Dasari, and M.S. Feld, "Single molecule detection using surface-enhanced Raman scattering (SERS)," *Phys. Rev. Lett.*, vol. 78, no. 9, pp. 1667–1670, Mar. 1997.

[6] S. Nie and S.R. Emory, "Probing single molecules and single nanoparticles by surface-enhanced Raman scattering," *Science*, vol. 275, no. 5303, pp. 1102–1106, Feb. 1997.

[7] M. Moskovits, "Surface-enhanced spectroscopy," *Rev. Mod. Phys.*, vol. 57, no. 3, pp. 783–826, July 1985.

[8] S.I. Bozhevolnyi, J. Beermann, and V. Coello, "Direct observation of localized second-harmonic enhancement in random metal nanostructures," *Phys. Rev. Lett.*, vol. 90, no. 19, art. no. 197403, May 2003.

[9] P.B. Johnson and R.W. Christy, "Optical constants of the noble metals," *Phys. Rev. B*, vol. 6, no. 12, pp. 4370–4379, 15 Dec. 1972.

[10] A.D. Rakic, A.B. Djurišic, J.M. Elazar, and M.L. Majewski, "Optical properties of metallic films for vertical-cavity optoelectronic devices," *Applied Optics*, vol. 37, no. 22, pp. 5271–5283, Aug. 1998.

[11] R. Gordon and A.G. Brolo, "Increased cut-off wavelength for a subwavelength hole in a real metal," *Optics Express*, vol. 13, no. 6, pp. 1933–1938, 21 Mar. 2005.

[12] M.I. Stockman, "Nanofocusing of optical energy in tapered plasmonic waveguides," *Phys. Rev. Lett.*, vol. 93, no. 13, art. no. 137404, 23 Sept. 2004.

[13] J.D. Jackson, *Classical Electrodynamics*. 3rd Ed. New York: Wiley, 1998.

[14] T. Okamoto, "Near-field spectral analysis of metallic beads," in *Near-Field Optics and Surface Plasmon Polaritons, Topics Appl. Phys.*, vol. 81, S. Kawata, Ed., Berlin: Springer-Verlag, 2001, pp. 97–123.

[15] K. Li and M.I. Stockman, and D.J. Bergman, "Self-similar chain of metal nanospheres as an efficient nanolens," *Phys. Rev. Lett.*, vol. 91, no. 22, art. no. 227402, 26 Nov. 2003.

[16] F.J. Garcia-Vidal, L. Martin-Moreno, E. Moreno, L.K.S. Kumar, and R. Gordon, "Transmission of light through a single rectangular hole in a real metal," *Physical Review B*, vol. 74, no. 15, art. no. 153411, 18 Oct. 2006.

[17] J. Homola, "Surface plasmon resonance sensors for detection of chemical and biological species," *Chem. Rev.*, vol. 108, no. 2, pp. 462–493, 30 Jan. 2008.

[18] A.J. Haes and R.P. Van Duyne, "A nanoscale optical biosensor: Sensitivity and selectivity of an approach based on the localized surface plasmon resonance spectroscopy of triangular silver nanoparticles," *J. Am. Chem. Soc.*, vol. 124, no. 35, pp. 10596–10604, 8 Aug. 2002.

[19] D.M. Schaadt, B. Feng, and E.T. Yu, "Enhanced semiconductor optical absorption via surface plasmon excitation in metal nanoparticles," *Appl. Phys. Lett.*, vol. 86, no. 6, art. no. 063106, 7 Feb. 2005.

[20] J.A.H. van Nieuwstadt, M. Sandtke, R.H. Harmsen, F.B. Segerink, J.C. Prangsma, S. Enoch, and L. Kuipers, "Strong modification of the nonlinear optical response of metallic subwavelength hole arrays," *Phys. Rev. Lett.*, vol. 97, no. 14, art. no. 146102, 6 Oct. 2006.

[21] J.B. Pendry, "Negative refraction makes a perfect lens," *Phys. Rev. Lett.*, vol. 85, no. 18, pp. 3966–3969, 30 Oct. 2000.

[22] N. Fang, H. Lee, C. Sun, and X. Zhang, "Sub-diffraction-limited optical imaging with a silver superlens," *Science*, vol. 308, no. 5721, pp. 534–537, 22 Apr. 2005.

[23] R. Merlin, "Radiationless electromagnetic interference: Evanescent-field lenses and perfect focusing," *Science*, vol. 317, no. 5840, pp. 927–929, 17 Aug. 2007.

[24] K.C. Neuman and S.M. Block, "Optical trapping," *Review of Scientific Instruments*, vol. 75, no. 9, pp. 2787–2809, Sept. 2004.

[25] M. Righini et al., "Surface plasmon optical tweezers: Tunable optical manipulation in the femtonewton range," *Phys. Rev. Lett.*, vol. 100, no. 18, May 2008.

[26] E.-S. Kwak, J. Henzie, S.-H. Chang, S.-K. Gray, G.C. Schatz, and T.W. Odom, "Surface plasmon standing waves in large-area subwavelength hole arrays," *Nano Letters*, vol. 5, no. 10, pp. 1963–1967, 2 Sept. 2005.

[27] W. Fan, S. Zhang, B. Minhas, K.J. Malloy, and S.R.J. Brueck, "Enhanced infrared transmission through subwavelength coaxial metallic arrays," *Phys. Rev. Lett.*, vol. 94, no. 3, art. no. 033902, 24 Jan. 2005.

ABOUT THE AUTHOR

Reuven Gordon (rgordon@uvic.edu) received his B.A.Sc. in engineering science and his M.A.Sc. in electrical engineering from the University of Toronto as well as a Ph.D. in physics from the University of Cambridge. In 2002, he joined the University of Victoria, where he currently holds an associate professor position in the Department of Electrical and Computer Engineering. He has authored and co-authored over 50 refereed journal papers, four invited papers, and one book chapter. He is the co-inventor of two patents, a Senior Member of the IEEE, and a Professional Engineer of BC.